



Excited state dynamics of β -carotene explored with dispersed multi-pulse transient absorption

Delmar S. Larsen ^{*}, Emmanouil Papagiannakis ^{*}, Ivo H.M. van Stokkum, Mikas Vengris, John T.M. Kennis, Rienk van Grondelle

Faculty of Sciences, Vrije Universiteit Amsterdam, De Boelelaan 1081, 1081 HV Amsterdam, The Netherlands

Received 27 August 2003; in final form 2 October 2003

Published online: 4 November 2003

Abstract

The excited-state dynamics of β -carotene in hexane was studied with dispersed ultrafast transient absorption techniques. A new excited state is produced after blue-edge excitation. Pump–repump–probe and pump–dump–probe measurements identified and characterized this state, termed S_1^\ddagger , which exhibits a blue-shifted spectrum with a longer lifetime than S_1 . We establish the independent co-existence of the S_1^\ddagger and S_1 states following the relaxation of S_2 and demonstrate that S_1^\ddagger is an electronically excited state and not a vibrationally excited ground-state species. Our data support the premise that S_1^\ddagger is formed directly from S_2 and not via preferential excitation of ground-state sub-populations.

© 2003 Elsevier B.V. All rights reserved.

1. Introduction

Carotenoids are natural pigments that play many important roles in photosynthesis, including the harvesting of sunlight and the transfer of energy to (bacterio) chlorophylls [1,2]. Their absorption of blue–green light corresponds to an electronic transition from the $1A_g^-$ ground state (S_0) to the $1B_u^+$ state (S_2). For symmetry reasons, the lower $2A_g^-$ state (S_1) cannot be directly accessed from S_0 by a one-photon absorption, though it can be populated after ultrafast (typi-

cally <200 fs) internal conversion from S_2 [2]. Early theoretical work on polyenes predicted the existence of additional ‘dark’ singlet states below S_2 [3] and recent experimental results have been presented supporting the existence of these states. Koyama and co-workers observed the $1B_u^-$ and the $3A_g^-$ states in different carotenoids with several spectroscopic techniques [4,5]. The observation of an additional intermediate transient state was also reported after S_2 relaxation in β -carotene and lycopene with high time-resolution transient absorption experiments [6]. Another excited state, of thus far unidentified symmetry properties, tentatively labeled S^* , was first found in spirilloxanthin in solution and bound to a LH1 complex [7] and was subsequently observed in other bacterial light-harvesting proteins [8]. However, incorporating

^{*} Corresponding authors. Fax: +31-20-444-7999. These authors contributed equally to this work.

E-mail addresses: dslarsen@nat.vu.nl (D.S. Larsen), papagian@nat.vu.nl (E. Papagiannakis).

these results into a consistent model of energy flow is not without difficulties, since multiple relaxation schemes have been proposed, each painting a complicated and different picture.

Understanding how carotenoids function in nature necessitates the study of excitation energy flow within their complicated electronic manifolds. This in turn requires the use of powerful spectroscopic techniques with both high time and wavelength resolution. Multi-pulse experiments have been successfully applied in studying complex dynamics not observed in pump–probe (PP) studies; in particular pump–dump–probe (PDP) and pump–repump–probe (PrPP) measurements have shown great potential. Ultrafast single-wavelength PDP experiments were used to study the elementary properties of the excited states in bacteriorhodopsin [9,10], and to explore ground state dynamics in calmodulin [11]; asymptotic-limited dispersed PDP has been used to study ground state liquid dynamics [12]. The higher excited-state dynamics of bacteriorhodopsin has been studied by single-wavelength PrPP [13], whilst the combined use of PDP and PrPP demonstrated overlapping bands in the PP signals [9]. Recently, we have used the dispersed PDP technique to investigate the dynamics of the ground state proton transfer in the green fluorescent protein [14] and the initiation dynamics of the photoactive yellow protein photocycle [15].

We applied dispersed multi-pulse techniques to study carotenoid dynamics in solution for the first time and this Letter outlines the results for β -carotene in hexane. The spectroscopic and dynamic properties of β -carotene have been extensively studied [16–18], we thus opt to use it as a model system to highlight the utility and power of multi-pulse techniques in dissecting and understanding the complicated carotenoid dynamics. Here, the term multi-pulse spectroscopy refers to signals collected with three pulses, two of high intensity and one low-intensity broadband probe pulse that is spectrally dispersed before detection. Depending on the timing and wavelength of the three pulses, different processes may be initiated, each exhibiting different dynamical and spectral properties. In our data, we can identify three distinct spectroscopic signals associated with different underlying

mechanisms: (1) PDP, (2) PrPP and (3) two-pulse two-photon absorption (2P2PA).

In the PDP signals, the first laser pulse excites the molecule and its excited state dynamics evolves naturally and unhindered until the application of a second pulse that transfers part of the excited population to the ground state. This requires the second laser pulse to be resonant with a stimulated emission (SE) band (Fig. 1C). Spectrally, PDP is observed as a decrease of any excited state absorption (ESA) and SE bands. Should the dumped population generate a non-equilibrated ground state species (e.g., thermally or structurally), then a positive band (often red-shifted from the ground state absorption) is generated, otherwise a uniform decrease of the bleach should be observed. The PDP technique, therefore, can directly probe the ground state dynamics of a non-equilibrated species.

If the second intense laser pulse is resonant with an ESA band, the observed effect is PrPP (Fig. 1B,D). The PrPP signals are the excited state

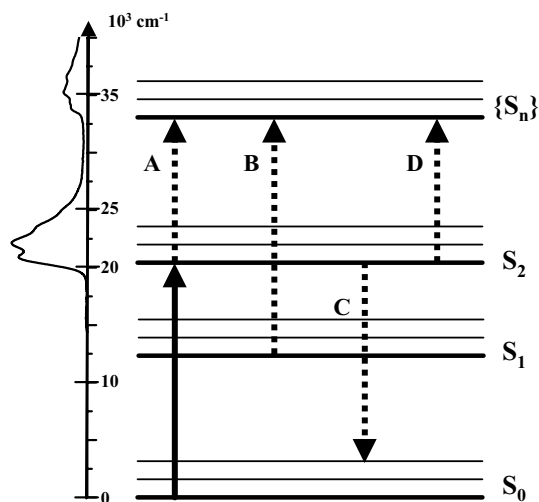


Fig. 1. Different multi-pulse processes observed in the β -carotene. For comparison, the one-photon absorption spectrum is displayed on the left of the figure. (A) 2P2PA process when the two pulses are temporally overlapped. (B) PrPP process with the $S_1 \rightarrow S_n$ transition. (C) PDP process with the $S_2 \rightarrow S_0$ transition. (D) PrPP process with the $S_2 \rightarrow S_n$ transition. The S_n electronic states accessed in the PrPP and 2P2PA processes need not necessarily be the same due to symmetry considerations of the electronic states and the two-photon transition selection rules.

analogue to the PDP signals and probe the redistribution of the excited state population within the excited state manifold, without involving of the ground state. Spectrally, these signals exhibit different signatures because of the nature of the properties of the initial and final excited states in the transition. In contrast to the PDP signals, the bleach is unaffected in the PrPP signals.

When both laser pulses are temporally overlapped and their combined energy is resonant with a higher electronic state, 2P2PA may occur, originating from the simultaneous absorption of both pulses (Fig. 1A). In contrast to the PDP and PrPP signals, 2P2PA leads to an additional excitation pathway resulting in both an increase of the bleach and excited state bands. In both the PrPP and 2P2PA mechanisms, the additional pumping of the molecules into higher electronic states introduces additional excitation energy into the system, which may generate high energy chemistry such as photo-ionization or photo-isomerization that is not observed with lower-energy excitation.

The identification and separation of the observed signals into these categories is an important prerequisite for the proper interpretation of such complex data. It is important to combine multi-pulse experiments with different wavelengths to highlight specific aspects of the underlying dynamics. The key in distinguishing these processes is the appropriate analysis of the complete information contained in the dispersed signals (i.e., changes in both bleach and excited state bands) often with the aid of global analysis methodologies [19,20].

2. Experimental details

2.1. Materials and experimental apparatus

All-*trans* β -carotene was purchased from Fluka and dissolved in *n*-hexane. The absorption spectra collected before and after each experiment show no sample degradation or the presence of isomeric impurities. The PP set-up described earlier [7] has been modified to include an additional pulse. The basis of the system is a 1-kHz amplified Ti:sapphire system (BMI α) delivering

450- μ J, 60-fs, 800-nm pulses. This output has been used in different ways to produce the wavelength combinations in the experiments described below. The dispersed multi-pulse experiments presented here involved laser pulses at four wavelengths: 400, 500, 530 and 800 nm. The 500- (588 cm^{-1} bandwidth) and 530-nm (500 cm^{-1} bandwidth) pulses were produced with a home-built non-collinear optical parametric amplifier, while a portion of the 800-nm light was doubled in a BBO crystal to provide the 400-nm (430 cm^{-1} bandwidth) pulses used for blue-wing excitation. In the 800-nm experiment, the pulses were used directly from the amplifier. The white-light continuum, used as a broad-band probe pulse, was generated by focusing a weak 800-nm beam into a slowly translating CaF_2 crystal. Reflective optics steered and focused the probe beam, reducing the group velocity dispersion to ~ 300 fs over 400–700 nm. A rapidly translating 1-mm quartz cuvette was used to hold the sample and two separate computer-directed translation stages controlled the time delays. The pump and dump/repump pulses were maintained at the same polarization and set at magic angle (54.7°) to the probe. The collected data have a wavelength and time resolution of 1 nm and 125 fs, respectively, with an average noise level of <1 mOD. Typical pulse intensities of the 400-, 500- and 530-nm pulses were ~ 150 nJ, whilst the 800-nm pulses were 500 nJ.

2.2. Action traces vs. kinetic traces

Traditional PP techniques involve the impinging of two short pulses (pump and probe) onto the sample, producing one-dimensional data. Two-dimensional information is extracted when the probe is a broad-band pulse that is dispersed onto a multi-channel detector. Introducing an additional pulse between the pump and the probe pulses generates three-dimensional signals (two time delays and one wavelength). The multi-dimensionality of these signals is exploited by measuring and presenting the data in various ways.

The most intuitive way to collect such three-dimensional data is in the form of a 'kinetic trace', where both the first and second laser pulses are set

at fixed times and the signals are collected by varying the probe pulse delay, as in PP experiments. However, the connectivity between transient states is often best studied in the form of an ‘action trace’. This is collected by delaying the second pulse with fixed pump and probe pulse times. By scanning the second pulse delay (with fixed probe time), the temporal efficiency of influencing the specific PP spectrum is directly monitored. Whilst kinetic traces directly monitor the dump/repump process, action traces measure their asymptotic effect at a specific probe time. In both modes, we construct the $\Delta\Delta\text{OD}$ signal which is the dump/repump induced change to the PP signals.

3. Results

3.1. Wavelength-dependent PP experiment

In order to investigate the role of the excitation wavelength on the excited state dynamics, we compare the PP signals collected after exciting β -carotene at the high- and low-energy sides of its S_2 absorption band (Fig. 1), with 400- (25 000 cm^{-1}) and 500-nm (20 000 cm^{-1}) pulses, respectively. Excitation-wavelength dependence of carotenoid PP dynamics has not been addressed in past studies, except for the case of peridinin [21].

Using the experimental setup described above for the multi-pulse experiments, we measured the two PP signals near-simultaneously (alternating every ~ 6 ms with mechanical choppers). The real-time collection of two different excitation PP signals guarantees identical experimental conditions, rejecting any potential errors due to sample degradation. Previous 500-nm excitation experiments on β -carotene show that after excitation into S_2 (Fig. 1), internal conversion moves population into a vibrationally ‘hot’ S_1 state within 200 fs [17]. The vibrational cooling of S_1 occurs on a sub-picosecond timescale resulting in a narrower ESA. The S_1 state then relaxes to the ground state with a lifetime of ~ 10 ps [18,22]. Similar spectroscopic and dynamical signals are also observed after 400-nm excitation, with small but clearly observable differences.

The 3-ps transient spectra, collected after thermalization of S_1 , for these two excitation wavelengths are contrasted in Fig. 2. Each spectrum exhibits strong ESA peaking at 550 nm, assigned to the $S_1 \rightarrow S_n$ transition. The 400-nm excited PP spectrum (solid curve) has a pronounced shoulder on the blue edge of the ESA that is nearly absent in the 500-nm excited spectrum. This spectral

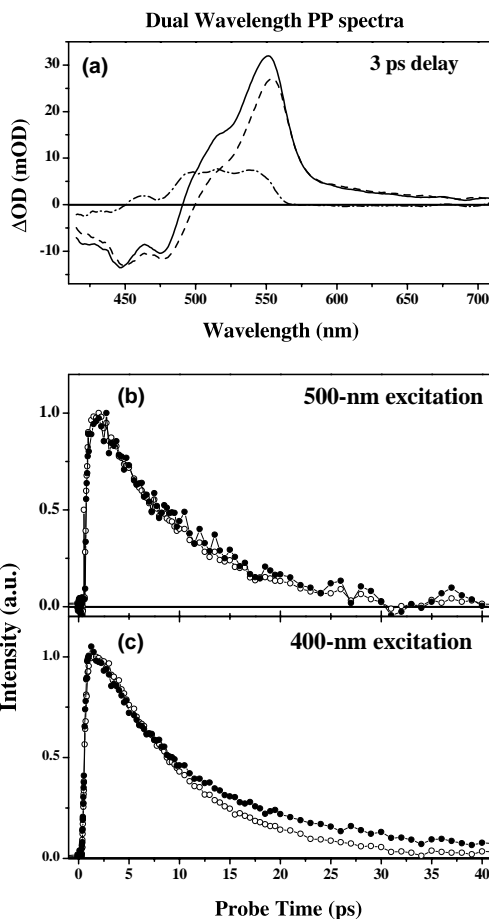


Fig. 2. Dual excitation PP transient signals. (a) Transient spectrum measured at 3 ps: 400-nm excitation (solid curve), 500-nm excitation (dashed curve) and the difference spectrum between the two (dot-dashed curve). The amplitude of the 500-nm spectrum is scaled (by 17%) to the 400-nm signal such that the bleach signals, at 450 nm, have equal magnitudes. (b) Normalized traces of the 500-nm excitation signals, measured at 510- (filled circles) and 550-nm (open circles). (c) Normalized traces of the 400-nm excitation signals measured at the same probe wavelengths. Same line demarcations as in panel b.

difference (dash-dot curve) can be described by the production of an additional and previously unobserved state that overlaps the S_1 state (dashed curve).

This new state, from here on referred to as S_1^\ddagger , exhibits distinctly different spectral and temporal properties from S_1 . Whilst the S_1 ESA peaks at 550 nm, S_1^\ddagger peaks further to the blue. The 500-nm excitation PP data exhibit a wavelength-independent decay [18], but the 400-nm excited spectrum evolves with slightly different, albeit discernible, wavelength-dependent dynamics (Fig. 2b,c). We postulate that this small temporal difference originates from the presence of S_1^\ddagger . Global fitting of both 400- and 500-nm excitation PP data (not shown) can separate this state from the other overlapping bands and show that S_1^\ddagger decays on two timescales: 10 and 65 ps (with $\sim 8\%$ amplitude). The first decay time is identical with the S_1 lifetime, but the latter decay time is clearly observed in Fig. 2c. It is tempting to relate this state to the S^* state [7], which bares certain similarities; we postpone this comparison to the discussion

section after more experimental results have been presented.

3.2. 800-nm PrPP experiment

The PP signals presented in Fig. 2 suggest the existence of an additional state that co-exists with S_1 . However, the identification of S_1^\ddagger as a separate state independent of S_1 is difficult from these data alone, because of the small spectral and temporal differences between the two states. To further confirm that these bands represent separate states, we contrast the results of two 800-nm PrPP experiments, with 400- and 500-nm excitation. In these experiments, after excitation, an 800-nm pulse repumps the excited state population into a higher electronic state. Since the S_1 ESA (Fig. 2a) exhibits a weak tail that extends beyond 800-nm [6] and the S_1^\ddagger absorption does not extend so far, then the 800-nm pulse will preferentially repump S_1 . The observation of a preferential repumping efficiency will establish these states as separate entities.

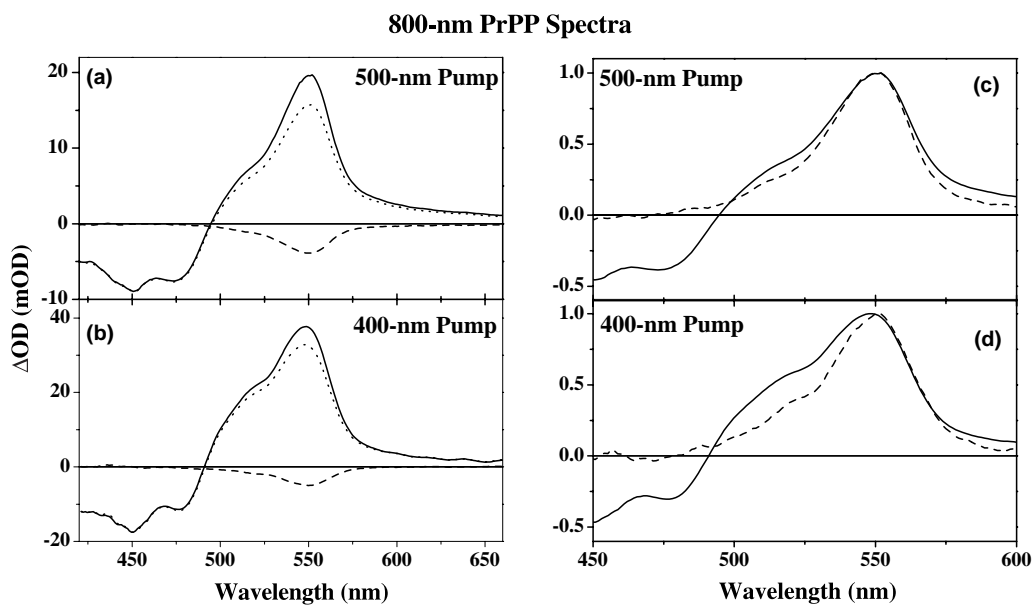


Fig. 3. PrPP spectra (800 nm). β -carotene was excited either at 400 or 500 nm and then interacted with 800-nm pulses. (a,b) Transient spectra measured with a probe time of 3 ps and a 800-nm delay at 1 ps. The PP spectrum (solid line), PP + 800-nm spectrum (dotted line) and 800-nm induced changes (dashed line). (c,d) Normalized PP spectra with the 800-nm induced changes. Same line demarcations as in panels a,b. Note that the Δ AOD spectra are inverted and re-scaled.

In Fig. 3, the transient spectra from the PrPP signals are shown with the probe pulse at 3 ps and the 800-nm pulse at 1 ps; the left panels contain the raw spectra, which are normalized to the ESA peak intensity in the right panels. As expected in PrPP signals, only the ESA is affected by the 800-nm pulse and the bleach is unaltered. Comparing the normalized $\Delta\Delta\text{OD}$ and PP spectra for the 500-nm excitation (Fig. 3c) shows that the 800-nm induces a homogeneous loss of ESA. In sharp contrast, after the 400-nm excitation, the loss is heterogeneous, as the additional S_1^\ddagger band observed in these PP spectra is effectively ‘untouched’ by the repump (Fig. 3d). The preferential depletion of S_1 over S_1^\ddagger demonstrates clearly that these states are distinct.

The 800-nm PrPP kinetic trace probed at 550 nm, after pumping at 400 nm and repumping at 300 fs (Fig. 4a), highlights the dynamics of the S_1 depletion. The population loss is instantaneous and persists during the lifetime of S_1 without exhibiting recovery dynamics. The relative population loss is time-independent and the dynamics observed in the $\Delta\Delta\text{OD}$ signal (filled triangles) only mirrors the S_1 population relaxation. The persistent loss is better observed in the action trace dynamics (Fig. 4b–d) which show the $\Delta\Delta\text{OD}$ signal increasing as the 800-nm pulse is delayed before attaining a constant level. This rise follows the decay of S_2 and hence the rise of the S_1 population. In contrast to the 400-nm excitation data, the action traces of the 500-nm excitation control experiment exhibit 2P2PA that obscures this rise (Fig. 4c,d). Despite this contamination, the long-time $\Delta\Delta\text{OD}$ spectra are unaffected by 2P2PA (Fig. 3a,c).

3.3. 530-nm PDP/PrPP experiment

The 800-nm PrPP experiments establish S_1^\ddagger as a separate state from S_1 , but shed little light on its nature. The similarity between S_1^\ddagger and the S_1 ESA does not necessarily imply that S_1^\ddagger is an electronically excited state and may instead correspond to a vibrationally excited or ‘hot’ electronic ground state rather than a true excited electronic state [23–25]. To address this issue, we performed an experiment where β -carotene was excited at 400

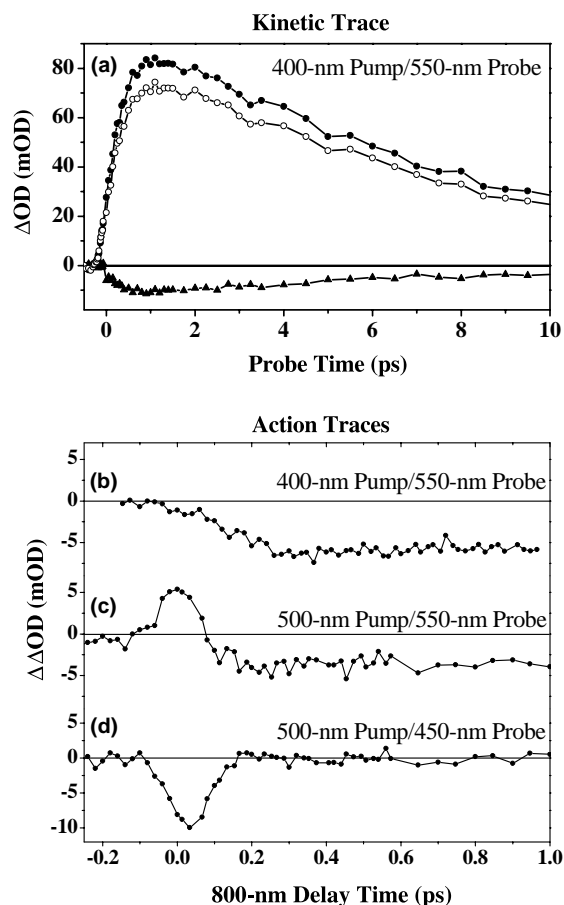


Fig. 4. PrPP traces (800 nm). β -carotene was excited either at 400 or 500 nm and then interacted with 800-nm pulses. (a) 550-nm Kinetic trace measured with an 800-nm delay time of 300 fs. The PP trace (filled circles), PP + 800-nm spectrum (unfilled circles) and 800-nm induced changes (filled triangles). (b–d) Action traces excited and measured at different wavelengths (see labels) with the probe time at 3 ps.

nm and subsequently interacted with a 530-nm pulse that is resonant with both the S_2 stimulated emission [17] and the S_1 ESA, but not with the ground state absorption (Fig. 1). Whilst S_2 is populated, the 530-nm pulse will dump S_2 to the ground state; if S_1 is populated, then its population will be repumped (Fig. 1). Should the S_1^\ddagger state be a ‘hot’ ground state species, then the controlled S_2 dumping with the 530-nm pulses should increase the signal of S_1^\ddagger and decrease the S_1 ESA.

These measurements are presented in Fig. 5, where panels a and b show that when the 530-nm

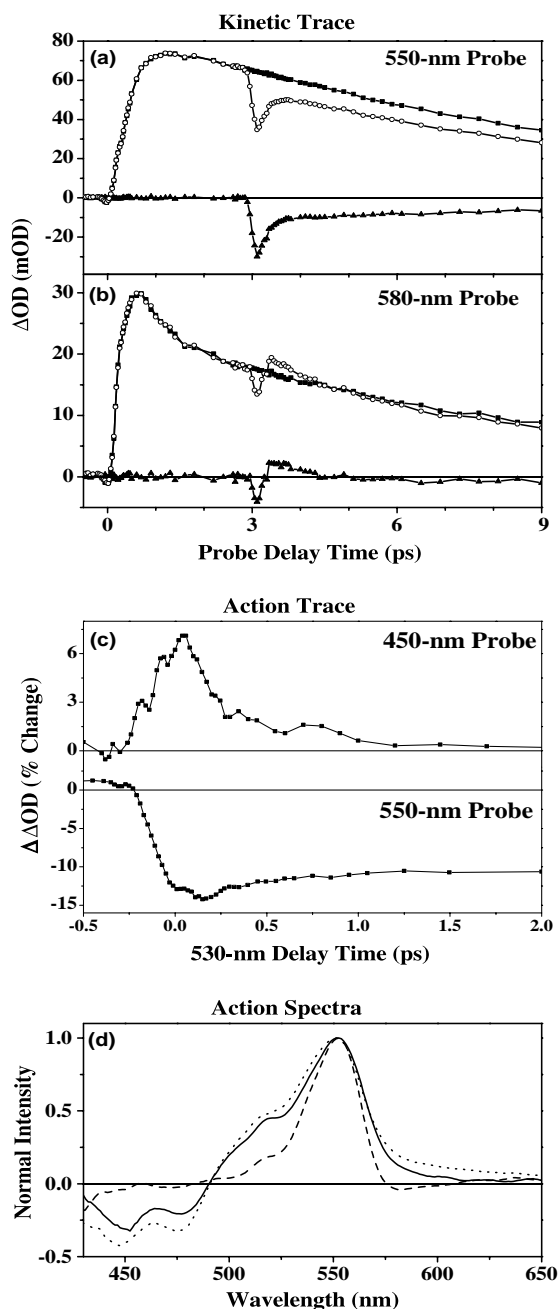


Fig. 5. Experiment (530 nm). β -carotene was excited at 400 nm and then interacted with 530-nm pulses. (a,b) Kinetic trace measured at 550 and 580 nm, with the 530-nm pulse at 3 ps. The same line demarcations as in Fig. 3a. (c) Action kinetics measured at 450 and 550 nm. (d) Normalized 3 ps PP spectrum (dotted line) and the negative Action-Spectra from global analysis: S_2 dump spectrum (300 fs), solid line, S_1 repump spectrum (10 ps), dashed line.

pulse is applied 3 ps after excitation, a significant portion of the S_1 ESA signal is instantaneously lost. The subsequent partial recovery in ~ 1 ps is attributed to the repopulation and vibrational relaxation of S_1 after decay of the higher electronic states. The dynamics probed at 580 nm (Fig. 5b) illustrate the vibrational relaxation of S_1 , where the repumped population (ESA decrease) returns via a transient hot S_1 state (ESA increase) before thermalization [18]. A persistent ESA loss, similar to the 800-nm repump data (Fig. 4a), is observed.

The action traces measured by varying the delay of the 530-nm pulse and probing at 3 ps display different dynamics when probing different bands. The bleach signal (Fig. 5c), measured at 450 nm, which probes the total excited population, shows a rapid loss (i.e., positive rise in the bleach $\Delta\Delta\text{OD}$ signal) when the 530-nm pulse is applied at early times and the dynamics directly follows that of S_2 . Concurrently, the ESA band, reflecting the S_1 population, exhibits a similar loss (i.e., negative rise in the ESA $\Delta\Delta\text{OD}$ signal) and the persistent loss observed in the kinetic trace (Fig. 5a). These observations confirm that the 530-nm pulses, in effect, dump the S_2 state to the ground state (Fig. 1c) during its lifetime, and afterwards repump S_1 (Fig. 5a,b). As expected for a PrPP process, only the ESA is affected, leaving the bleach untouched (Fig. 5c).

A global analysis of the $\Delta\Delta\text{OD}$ action traces is used to extract the complete spectral changes associated with the aforementioned signals. The resulting fitted Action-Spectra describe the spectral changes associated with a specific decay lifetime in the data [19,20]. The analysis of the 530-nm action traces shows two sequential components of ~ 300 fs (PDP) and ~ 10 ps (PrPP), corresponding to the lifetimes of the S_2 and S_1 states, respectively (Fig. 5d). The estimated late-time PrPP Action-Spectrum (dashed line) exhibits no change in the bleach region, corresponding to a process that does not involve the ground state, i.e., a repump process, and is near-identical to the $\Delta\Delta\text{OD}$ spectra observed in the 800-nm PrPP experiment (Fig. 3c,d), further demonstrating the separation of the S_1 and S_1^\ddagger states.

In stark contrast, the early-time PDP Action-Spectrum (Fig. 5d, solid curve) exhibits significantly

different properties. A distinct bleach structure is observed, confirming the loss of excited population, i.e., a dump, which occurs when the 530-nm pulse is applied whilst S_2 is populated. As expected for a dumping process, we observe a concomitant decrease in the ESA. The PDP Action-Spectra are nearly indistinguishable from the PP spectrum (Fig. 5d, dotted curve), confirming that S^\ddagger is lost in the dumping process and therefore evolves directly from S_2 .

4. Discussion

Our multi-pulse experiments show that when β -carotene is excited on the high-energy side of S_2 , an additional relaxation pathway is activated generating a transient species, S^\ddagger , which is disconnected from S_1 and is blue-shifted compared to it (Fig. 2).

Despite the similar underlying repumping mechanisms, a clear difference is observed between the 530- and 800-nm PrPP signals (Figs. 4a and 5a,b). Once population is repumped into S_n , rapid internal conversion brings it back to lower electronic states as observed in other PrPP experiments [9,13]. The 530-nm repump experiment (Fig. 5a,b) highlights this relaxation as the re-excited population evolves from S_n through S_2 and hot S_1 before eventually reaching the relaxed S_1 . However, only part of the repumped population follows this scheme and the rest ‘disappears’. The 800-nm PrPP data (Fig. 4a) show no population recovery, but instead exhibit only a persistent loss. A potential explanation would be a resonantly enhanced two-photon ionization mechanism, where the accessed higher electronic state is strongly coupled to a continuum state, generating an ejected electron and a carotenoid radical [26]. Since neither the radical nor the ejected electron absorb in the spectral window of the experiments presented here [27], this mechanism would in effect appear as a population loss.

An alternative hypothesis is that the repump pulse redistributes population into a ‘dark’ or low-extinction state that is not clearly observed in our data. A measurement of the PrPP $\Delta\Delta\text{OD}$ signal as a function of the 800-nm pulse power showed a near-linear trend expected from one-photon tran-

sitions. Despite the uncertain origin of this population loss, both 800- and 530-nm PrPP experiments clearly distinguish the existence of two co-existing transient states after 400-nm excitation of β -carotene. The nature of this depletion does not alter the observation and characterization of the S^\ddagger state, which is the crux of this Letter.

Two different mechanisms can explain the observation of S^\ddagger in the excitation wavelength dependent PP data (Fig. 2): (A) branched relaxation from S_2 or (B) ground-state inhomogeneity. The first hypothesis postulates an excitation wavelength dependent decay channel of S_2 that results in the simultaneous formation of S^\ddagger and S_1 . The second suggestion proposes the co-existence of several ground state sub-populations with the molecules exhibiting S^\ddagger -like features being preferentially excited by the 400-nm excitation.

The PDP results show a depletion of both S_1 and S^\ddagger after the S_2 dumping (Fig. 5d), directly supporting the branched model. On the contrary, explaining these data with the ground-state inhomogeneity hypothesis requires the assumption of near-identical dumping efficiencies of the S_2 states in each of the sub-populations. This assumption seems unlikely, because the other properties of the supposed sub-populations, like the ground-state absorption bands (blue edge vs. red edge) and the ESA bands (S^\ddagger vs. S_1) are rather dissimilar. We favor the more straightforward branching scenario to explain the generation of S^\ddagger , since it is improbable that the dumping efficiencies of the different sub-populations S_2 states are identical.

The observation of the S^\ddagger state is not unique to β -carotene, (results will be discussed elsewhere), but is also seen in other highly purified (via HPLC) carotenoid samples including: neurosporene, spheroidene, lycopene and spirilloxanthin. This further disfavors the argument that S^\ddagger originates from ground state inhomogeneity.

It has been suggested that the blue shoulder of the S_1 ESA band, corresponding to the S^\ddagger state in our measurements, is not an electronically excited state as S^* , but instead is a ‘hot’ ground electronic state [24,25]. It is further suggested that this state is generated via an impulsive stimulated Raman scattering (ISRS) mechanism with a broad band excitation pulse [23]. However, Fig. 5d clearly

demonstrates that when S_2 is dumped, the $\Delta\Delta OD$ loss spectrum is near-identical with the PP spectrum and no increase of the S^{\ddagger} band is observed. Hence, the $\sim 6000\text{ cm}^{-1}$ energy (difference between 400-nm pump and the 530-nm dump pulses) is insufficient to generate a noticeably red-shifted hot band. Conclusively, the S^{\ddagger} state is not a ground state species, but is an excited state and ISRS is not an appreciable mechanism in these experiments. This is further corroborated with the observation of a similar long-lived species found after narrow-band excitation of β -carotene [28].

At first glance S^{\ddagger} is not so dissimilar from the S^* state, which was observed in spirilloxanthin and has similar properties; however as mentioned earlier, S^* is created after red-wing excitation and moreover its ESA is not as blue-shifted and broad as that of S^{\ddagger} [7,8]. S^* has a 5-ps lifetime without a long-living component and moreover it was identified as a triplet precursor and energy donor in light-harvesting complexes [8]. Finally, 400-nm excitation PP measurements on spirilloxanthin indicate that S^* and S^{\ddagger} are different excited species and that S^{\ddagger} is a product of high-energy excitation, probably a property common among carotenoids.

Earlier experiments on β -carotene with 355-nm excitation pulses [28] resulted in the generation of a similar long-lived transient species which was not observed with red-edge excitation [18]. Additionally, fluorescence-excitation studies on several carotenoids show that excitation on the blue side of the S_2 absorption band often results in decreased fluorescence suggesting the presence of the additional pathway [29].

The nature of the S^{\ddagger} and S^* states remains uncertain. Calculations on polyenes [3] predict two electronic states, apart from S_1 , under S_2 , the $1B_u^-$ and the $3A_g^-$ states. However, in order to assign the observed S^{\ddagger} (or S^*) to any of them, determination of their 0–0 energy is required. It is also unclear to what degree does the configuration of carotenoids influence their excited-state manifold. It has been proposed that the relaxation in the excited state manifold of β -carotene includes minor structural changes [18] and that in light-harvesting complexes, the protein-imposed configuration controls an additional deactivation channel [30]. Thus, we speculate that S^{\ddagger} may result

from overcoming a configurational barrier in S_2 when excited with additional energy.

5. Conclusions

Several ultrafast dispersed multi-pulse experiments were used to investigate the excitation relaxation dynamics of β -carotene in hexane by explicitly manipulating transient electronic state populations with the application of carefully tuned (both spectrally and temporally) laser pulses. Three experiments were performed involving the application of a pair of laser pulses of differing wavelengths and a broad-band probe pulse: (1) 400-/500-nm wavelength-dependent PP. (2) 400- (and 500-)/800-nm PrPP and (3) 400-/530-nm PDP/PrPP.

This combination of powerful multi-pulse techniques enabled us to identify and characterize an additional electronic energy relaxation pathway opening when the β -carotene is excited with excess electronic energy. This leads to the formation of a transient state, S^{\ddagger} , that co-exists and evolves in parallel with the S_1 electronic state. The PrPP experiment illustrates clearly the co-existence of S^{\ddagger} and S_1 , whilst the PDP experiment shows that S^{\ddagger} is a true electronically excited state (albeit with a longer lifetime than the S_1 state) and should not be confused with a ‘hot’ ground state species.

The relationship between S^{\ddagger} and S^* , which has been definitively observed only for spirilloxanthin in solution and for more carotenoids bound to light-harvesting complexes [7,30], is still uncertain. However, the results of a more detailed multi-pulse spectroscopic study in progress, including global analysis, that compares the PDP and PrPP signals of different carotenoids, including spirilloxanthin [31], imply that S^{\ddagger} is not related to S^* .

Acknowledgements

This research was supported by the Netherlands Organization for Scientific Research (NWO) via the Dutch Foundation for Earth and Life Sciences (ALW). D.S.L. is grateful to the Human Frontier Science Program Organization for providing financial support with a long-term fellowship. J.K.

acknowledges financial support from the Foundation for Fundamental Research on Matter (FOM).

References

- [1] H.A. Frank, R.J. Cogdell, Photochemistry and photobiology 63 (1996) 257.
- [2] T. Ritz, A. Damjanovic, K. Schulten, J.P. Zhang, Y. Koyama, Photosynthesis Research 66 (2000) 125.
- [3] P. Tavan, K. Schulten, Journal of Chemical Physics 85 (1986) 6602.
- [4] R. Fujii, T. Inaba, Y. Watanabe, Y. Koyama, J.P. Zhang, Chemical Physics Letters 369 (2003) 165.
- [5] F.S. Rondonuwu, Y. Watanabe, R. Fujii, Y. Koyama, Chemical Physics Letters 376 (2003) 292.
- [6] G. Cerullo, D. Polli, G. Lanzani, S. De Silvestri, H. Hashimoto, R.J. Cogdell, Science 298 (2002) 2395.
- [7] C.C. Gradinaru, J.T.M. Kennis, E. Papagiannakis, I.H.M. van Stokkum, R.J. Cogdell, G.R. Fleming, R.A. Niederman, R. van Grondelle, Proceedings of the National Academy of Sciences of the United States of America 98 (2001) 2364.
- [8] E. Papagiannakis, J.T.M. Kennis, I.H.M. van Stokkum, R.J. Cogdell, R. van Grondelle, Proceedings of the National Academy of Sciences of the United States of America 99 (2002) 6017.
- [9] F. Gai, J.C. McDonald, P. Anfinrud, Journal of American Chemical Society 119 (1997) 6201.
- [10] S. Ruhman, B. Hou, N. Freidman, M. Ottolenghi, M. Sheves, Journal of American Chemical Society 124 (2002) 8854.
- [11] P. Changenet-Barret, C. Choma, E. Gooding, W. DeGardo, R.M. Hochstrasser, Journal of Physical Chemistry B 104 (2000) 9322.
- [12] S.A. Kovalenko, J. Ruthmann, N.P. Ernsting, Journal of Chemical Physics 109 (1998) 1894.
- [13] S.L. Logunov, V.V. Volkov, M. Braun, M.A. El-Sayed, Proceedings of the National Academy of Sciences of the United States of America 98 (2001) 8475.
- [14] J.T.M. Kennis, D.S. Larsen, I.H.M. van Stokkum, M. Vengris, J.J. van Thor, R. van Grondelle (submitted).
- [15] D.S. Larsen, I.H.M. van Stokkum, M. Vengris, M. van der Horst, K. Hellingwerf, R. van Grondelle (submitted).
- [16] A.P. Shreve, J.K. Trautman, T.G. Owens, A.C. Albrecht, Chemical Physics Letters 178 (1991) 89.
- [17] H. Kandori, H. Sasabe, M. Mimuro, Journal of the American Chemical Society 116 (1994) 2671.
- [18] F.L. de Weerd, I.H.M. van Stokkum, R. van Grondelle, Chemical Physics Letters 354 (2002) 38.
- [19] A.R. Holzwarth, in: J. Ames, A.J. Hoff (Eds.), Biophysical Techniques in Photosynthesis, Kluwer Academic Publishers, Dordrecht, 1996.
- [20] I.H.M. van Stokkum, R.H. Lozier, Journal of Physical Chemistry B 106 (2002) 3477.
- [21] D. Zigmantas, R.G. Hiller, A. Yartsev, V. Sundström, T. Polívka, Journal of Physical Chemistry B 107 (2003) 5339.
- [22] H.H. Billsten, D. Zigmantas, V. Sundstrom, T. Polívka, Chemical Physics Letters 355 (2002) 465.
- [23] J. Savolainen, T. Buckup, W. Wohlleben, J. Herek, H. Hashimoto, R.J. Cogdell, M. Motzkus, Femtochemistry IV, Paris, 2003; poster No. P55II.
- [24] P.O. Andersson, T. Gillbro, Journal of Chemical Physics 103 (1995) 2509.
- [25] M. Yoshizawa, H. Aoki, H. Hashimoto, Physical Review B 63 (2001) 180301.
- [26] W. Ryan, D.J. Gordon, D.H. Levy, Journal of American Chemical Society 124 (2002) 6194.
- [27] J.A. Jeevarajan, C.C. Wei, A.S. Jeevarajan, L.D. Kispert, Journal of Physical Chemistry 100 (1996) 5637.
- [28] H. Hashimoto, Y. Koyama, Y. Hirata, N. Mataga, Journal of Physical Chemistry 95 (1991) 3072.
- [29] B. Decoster, R.L. Christensen, R. Gebhard, J. Lugtenburg, R. Farhoosh, H.A. Frank, Biochimica Et Biophysica Acta 1102 (1992) 107.
- [30] E. Papagiannakis, S.K. Das, A. Gall, I.H.M. van Stokkum, B. Robert, R. van Grondelle, H.A. Frank, J.T.M. Kennis, Journal of Physical Chemistry B 107 (2003) 5642.
- [31] E Papagiannakis, oral presentation, Femtosecond Dynamics in Photosynthetic Light Harvesting Complexes, Antalya, Turkey, 2002.